ISBN: 978-3-95450-247-9 ISSN: 2673-5490 doi: 10.18429/JACoW-IPAC2024-WEPS63

MECHANICAL DESIGN OF THE 12 T SUPERCONDUCTING DIPOLE. AN ACCELERATOR-FIT Nb_3Sn DOUBLE APERTURE MAGNET

M. Masci*, L. Baudin, D. Perini, European Organization for Nuclear Research, Meyrin, Switzerland

Abstract

In the context of the High Field Magnet programme [1], the 12 T Nb_3Sn activity aims to design and manufacture a 2-meter-long, 12 T, cosθ, double aperture dipole. To reach magnetic fields higher than 10 T in accelerator magnets, brittle epoxy-impregnated Nb_3Sn Rutherford cables are employed, which makes it difficult to predict the coil's mechanical limit and, in extenso, the magnet's performance. To tackle this challenge, expensive procedures are often implemented. The 12 T mechanical design presented in this paper aims to prioritize intrinsically safe structures and minimize the number of components. This approach is intended to counteract issues stemming from fabrication tolerances and assembly tool misalignment. To prevent coil over-compression, mechanical stoppers are integrated within the magnet structure. The design is committed to focus on solutions that can be applied on short demonstrators but also scaled to long magnets that need to be produced in large quantities in series. This paper aims to introduce the magnet's mechanical design, its underlying principles, and the advantages it offers.

INTRODUCTION

Since the 1970s, the field requirements for superconducting dipoles in accelerators have significantly increased, resulting in the necessity to design coils and support structures able to withstand electromagnetic forces ten times larger with respect to the past generation magnets, while employing mechanically much less forgiving materials than Nb-Ti [2]. Any design of an accelerator fit dipole must have in mind large-scale production, which requires adherence to industrial standards and economic viability, calling for simplified processes and reasonable components tolerances. During assembly, efforts are made to align parts closely to nominal requirements, but fabrication tolerances, thermal contraction, and electromagnetic forces can affect resulting contact forces, requiring designers to assess operational viability within tolerance ranges and consider adjustments. Often to achieve high performances on prototypes, extremely tight tolerances are enforced, and labor-intensive procedures are employed, which do not provide a solution for the final design goal: a large-scale production of a long magnet. By minimizing the number of components, limiting the requirement for tight tolerances to a few strategic surfaces, and implementing compensation shims based on measured deviations, the designers can significantly simplify the assembly processes [3–5]. The goal of this paper is to describe a mechanical design solution for a 12 T, cosθ, double aperture dipole that puts as its base economic viability and ease of assembly.

* marco.masci@cern.ch

INTRINSICALLY SAFE STRUCTURE: USE OF MECHANICAL STOPPERS

A way to build a mechanically intrinsically safe structure is to work displacement imposed instead of force imposed. The design goal is to protect the coils in each step of the assembly by limiting the effect that any imbalance in the load could have on the coils and mitigating accidental peak stresses. In each assembly step, a component should always fulfill the role of load aligner and coil protector. Figure 1 illustrates this concept. In the figure, the coils are depicted in blue and straightened and of nominal dimension for simplicity. The rigid component acting as a protector is shown in grey, while an uneven pressure generated by an accidental misalignment is highlighted in red.

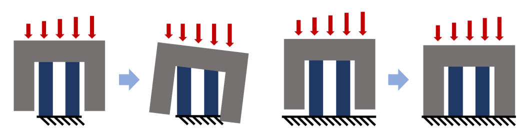

Figure 1: On the left, when the misalignment occurs, the rigid component transmits the imbalanced force to the coils, causing one coil to compress much more than the other. On the right, a mechanical stopper is present: the rigid component and the stoppers create a closed cavity. After an initial imbalanced phase, once the gap is closed, the load on the coils is equal on both sides.

Assembly Procedure

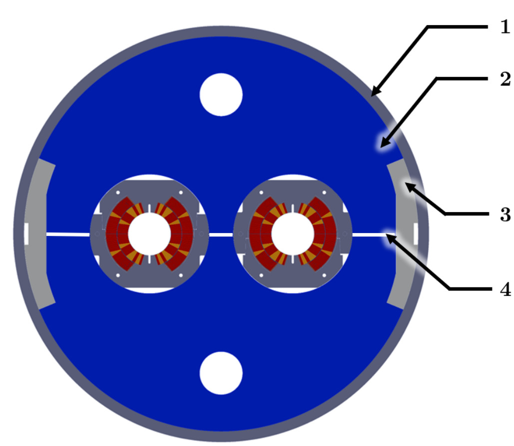

Figure 2: Magnet cross-section: (1) Stainless steel shell. (2) Iron yoke. (3) Lateral aluminum stoppers. (4) Horizontal yoke split.

© Content from this work may be used under the terms of the CC BY 4.0 licence (© 2024). Any distribution of this work must maintain attribution to the author(s), title of the work, publisher, and DOI.

ISBN: 978-3-95450-247-9 ISSN: 2673-5490 doi: 10.18429/JACoW-IPAC2024-WEPS63

Content from this work may be used under the terms of the CC BY 4.0 licence (© 2024). Any distribution of this work must maintain attribution to the author(s), title of the work, publisher, and DOI.

Figure 3 shows the assembly steps to achieve the cross-section depicted in Figure 2. The cold mass assembly process begins by positioning the collared coils on the bottom yoke half. Subsequently, the second yoke half is placed on top. To ensure proper alignment and to enforce the necessary gap in the yoke horizontal split, two aluminum lateral stoppers are positioned between the yoke halves at their sides. Once the second half of the stainless-steel shell is positioned, the assembly is prepared for welding. During the welding process, an azimuthal stress is generated on the shell, causing the two yoke halves to be pushed together. As a result, the yoke exerts pressure on the aluminum stoppers and the collared coils. The aluminum stoppers and the collared coils work as springs in parallel, with the aluminum stoppers protecting the coils from overloading. At cold, the top faces of the aluminum stoppers, given aluminum's higher coefficient of thermal expansion with respect to the other components [6], lose contact with the iron yoke, making the aluminum stoppers effectively 'disappearing', allowing the forces that were previously acting on them to be transferred to the coils. The amount of force that can be exchanged between the yoke and the coils is limited by the size of the yoke split. Once the two yoke halves are in contact, the collared coils and the yoke work as springs in parallel, with the yoke now preventing coils from overloading given its higher stiffness.

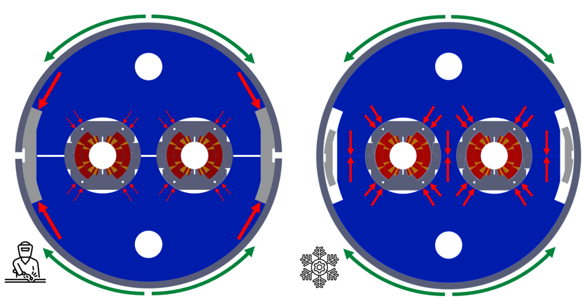

Figure 3: Assembly steps overview. The red arrows show how the contact forces are exchanged between the components. On the left during welding and on the right at cold. The green arrow represents the azimuthal stress on the shell due to welding.

RECOVERING PRESTRESS AT COLD IN A COLLARED COIL MAGNET: HORIZONTAL YOKE SPLIT

The presence of a horizontal yoke split allows to gain prestress on the coils during welding and cooling. This represents a difference from the vertical split yoke magnets like LHC dipoles [7] or HL-LHC 11 T [8]. Figure 4 shows that the maximum pole-coil prestress is achieved under the collaring press, and subsequent steps result in a loss of prestress. With the system's capability to gain prestress, there is no longer a need to employ thick collars to counteract the spring-back effect post-collaring. This design is compatible with thin collars, enabling the placement of iron as close as possible to the coils. Moreover, the presence of a stainless-steel cylindrical shell allows for the use of end plates fixed to it and retaining bolts. This gives the shell the role of structural stiffener against longitudinal electromagnetic forces. With this configuration no tie rods are needed, making it easier to scale the design from a short demonstrator to an accelerator magnet.

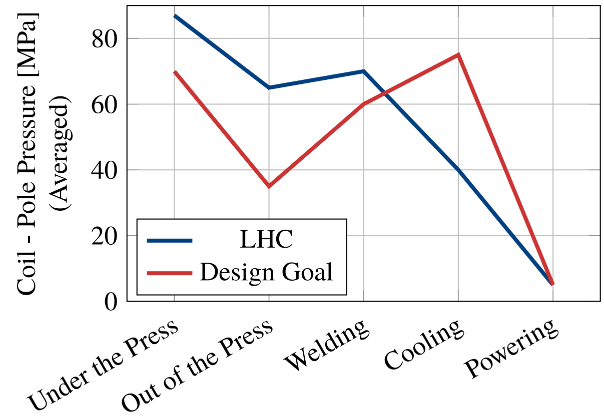

Figure 4: Comparison between a standard collared magnet [7] and the proposed design.

CORRELATION BETWEEN COIL HORIZONTAL DISPLACEMENT AND ITS AZIMUTHAL PEAK STRESS

A horizontally split iron yoke has another valuable advantage: its shape has no discontinuities in the direction of Lorentz forces (horizontal when looking at a cross-section). The yoke's continuity in this transversal direction provides stiffness at powering, so the structure deformations are less sensitive to material, thickness, and preload of the external shell.

The advantage of a stiff structure can be seen by computing how the magnet rigidity affects the coils' azimuthal peak stress. On the midplane at the bore inner radius for a sector coil housed in an infinitely rigid structure the azimuthal stress is given by [9]:

$$\sigma_\theta = \frac{B^2}{2\mu_0}\frac{\pi}{\sqrt{3}}\frac{(\text{Inner Radius})}{(\text{Coil Thickness})} \tag{1}$$

The result changes significantly when the cavity that houses the coil is no longer perfectly rigid. To compute the peak stress, solely due to electromagnetic forces, for a sector coil (inner radius = 25 mm, coil thickness = 36 mm) generating a field of 12 T housed in a deformable structure, a finite element analysis has been performed. The material properties for the coil are assumed to be linear elastic (E = 40 GPa, $\nu = 0.3$), and the contact between the coil and the housing frictionless.

Figure 5 shows that the maximum stress seen by the coil when housed in a structure that allows a horizontal displace-

ISBN: 978-3-95450-247-9 ISSN: 2673-5490 doi: 10.18429/JACoW-IPAC2024-WEPS63

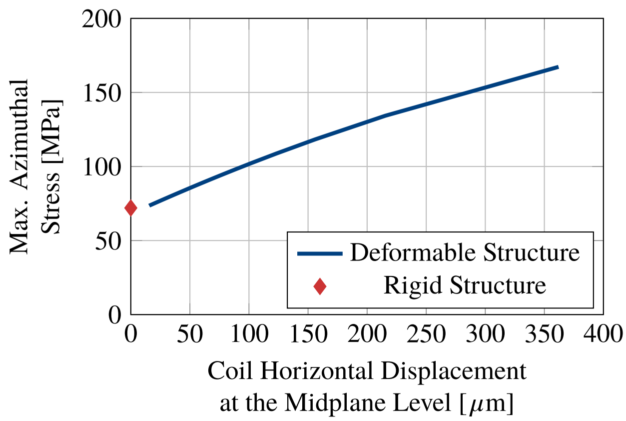

Figure 5: Effect of the coil housing displacement on the coil peak azimuthal stress.

ment of 150 μm, is 37% higher than when the displacement is limited to 50 μm. Minimizing displacement in the structure is one of the first goals of this magnet mechanical design.

COMPONENT COUNT MINIMIZATION

Mass production of machined components often gives parts with Gaussian distributions of dimensions, with different averages but similar standard deviations, mainly correlated to the fabrication technology [10]. Assembling components implies dealing with tolerance ranges at every interface. The sum of independent Gaussian distributions is also a Gaussian distribution, and its variance can be calculated using the central limit theorem [11]. There are two ways to reduce the effect of tolerances: the first one is to reduce the width of each tolerance range. Nevertheless, tight tolerances are not always achievable and imply costs, delays in fabrication, and extra steps in quality control. The second is to reduce the number of pieces. A design oriented to this goal can significantly reduce the effect generated by stacking up tolerances.

Tolerances on the aluminium stoppers size have a reduced impact for two reasons. The first one is their position at the side of the magnet, where a linear deviation in their size generates a small angular deviation of the yoke. The second one is that at cold, any imbalance in the stoppers will not pile up with the yoke's tolerances, since the stoppers' top face will lose contact with the yoke during cooldown.

Effect of Tolerances

A simplified analysis can be conducted to estimate how the tolerances affect the stress change after cooling. All the components are straightened. Linear elastic properties are assumed for the coils (20 GPa) while the others are considered rigid. The real size of the collared coils and the yoke will be reflected in the total size of the yoke gap.

Figure 6 shows three stages:

I The gap is too small to have any effect on the collared coil. The coil loses compression while cooling

II The gap is big enough to compress the coil while cooling. The amount of the compression depends on the size of the yoke gap. The two yoke halves form a cavity while cooling.

III The yoke gap remains open at cold. The stoppers never lose contact with the yoke and any increase in the size of the yoke gap has no effect on the stress on the coils.

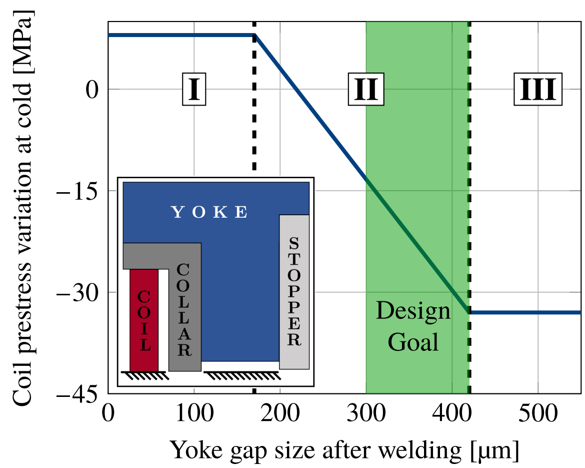

Figure 6: Effect of the yoke gap on the coil prestress after cooling, simplified analysis. The green area gives the tolerance range for the yoke gap. This value is close to the yoke size tolerances for LHC dipoles [12].

CONCLUSIONS

In this paper, we have presented a mechanical design solution for a 12 T, 2-in-1, cosθ, dipole accelerator magnet, prioritizing mechanical design solutions in line with large-scale production. Key challenges were addressed, such as: coil stress management, tolerances, and structural stiffness. The proposed design offers several advantages. The reduction of the number of components mitigates the complexities associated with the control of tolerance ranges for different interfaces. This streamlines the assembly process and minimizes average deviations. The design incorporates the use of collared coils into a horizontally split yoke together with aluminum stoppers. This approach enables to gain prestress on the coils during the cold mass assembly and cooldown. At the same time, it removes the need for thick collars and allows for closer placement of iron to the coils. An iron yoke with a horizontal split provides enough stiffness to limit the coil displacement during powering and subsequently its peak stress. A dedicated development program is currently ongoing at CERN to address the production challenges and validate the design via mockup testing.

REFERENCES

[1] P. Védrine *et al.*, "High-field magnets," *CERN Yellow Reports: Monographs*, Vol. 1: European Strategy for Particle Physics-

© Content from this work may be used under the terms of the CC BY 4.0 licence (© 2024). Any distribution of this work must maintain attribution to the author(s), title of the work, publisher, and DOI.

ISBN: 978-3-95450-247-9 ISSN: 2673-5490 doi: 10.18429/JACoW-IPAC2024-WEPS63

Accelerator R&D Roadmap, Mar. 2022. doi:10.23731/CYRM-2022-001.9.

[2] S. Caspi and P. Ferracin, "Limits of Nb3Sn accelerator magnets", in *Proc. PAC'05*, Knoxville, TN, USA, May 2005, paper TOAA001, pp. 107–111. doi:10.1109/PAC.2005.1590372.

[3] L. Rossi, "The LHC main dipoles and quadrupoles toward series production," *IEEE Transactions on Applied Superconductivity*, vol. 13, no. 2, pp. 1221–1228, Jun. 2003. doi:10.1109/tasc.2003.812639

[4] L. Rossi, "Experience with LHC Magnets from Prototyping to Large-scale Industrial Production and Integration", in *Proc. EPAC'04*, Lucerne, Switzerland, Jul. 2004, paper WEXCH01, pp. 118–122.

[5] A. Devred *et al.*, "About the mechanics of SSC dipole magnet prototypes," *AIP Conference Proceedings*, Jan. 1992. doi:10.1063/1.41955

[6] C. Kokkinos, "Material properties used in FE models", EDMS CERN Portal, Document ID 2002489 v.1.

[7] P. Fessia, *et al.*, "Selection of the cross-section design for the LHC main dipole," *IEEE Transactions on Applied Superconductivity*, vol. 10, no. 1, pp. 65-–68, Mar. 2000. doi:10.1109/77.828177

[8] B. Bordini *et al.*, "Nb_3Sn 11 T dipole for the high luminosity LHC (CERN)", *Particle Acceleration and Detection*, pp. 223-–258, 2019. doi:10.1007/978-3-030-16118-7_9.

[9] M. N. Wilson, *Superconducting Magnets*. Oxford University Press, 1987.

[10] P. J. Drake, *Dimensioning and tolerancing handbook*, New York: Mcgraw Hill, 1999.

[11] H. Cramér, *Mathematical methods of statistics*, Princeton: Princeton University Press, 1999.

[12] P. Fessia, *et al.*, "Comparative study of different designs of the mechanical structure for the LHC main dipoles". CERN, Geneva, Switzerland, No. LHC-PROJECT-NOTE-288, 2002.

© Content from this work may be used under the terms of the CC BY 4.0 licence (© 2024). Any distribution of this work must maintain attribution to the author(s), title of the work, publisher, and DOI.